DOI: 10.1002/chem.200601211

The First Pure ΛHT Rotamer of a Complex with a *cis*-[Metal(nucleotide)$_2$] Unit: A *cis*-[Pt(amine)$_2$(nucleotide)$_2$] ΛHT Rotamer with Unique Molecular Structural Features

Michele Benedetti,[b] Gabriella Tamasi,[c] Renzo Cini,[c] Luigi G. Marzilli,[d] and Giovanni Natile*[a]

Abstract: *cis*-[PtA$_2$(nucleotide)$_2$] complexes (A$_2$ stands for two amines or a diamine) have been extensively investigated as model compounds for key cisplatin–DNA adducts. All *cis*-[metal(nucleotide/nucleoside)$_2$] complexes with guanine and related purines characterized in the solid state thus far have the ΔHT conformation (head-to-tail orientation of the two bases and right-handed chirality). In sharp contrast, the ΛHT conformation (left-handed chirality) dominates in acidic and neutral aqueous solutions of *cis*-[PtA$_2$(5′-GMP)$_2$] complexes. Molecular models and solution experiments indicate that the ΛHT conformer is stabilized by 5′-phosphate/N1H hydrogen-bond interactions between *cis* nucleotides with the normal *anti* conformation. However, this evidence, while compelling, is indirect. At last, conditions have been defined to allow crystallization of this elusive conformer. The structure obtained reveals three unique features not present in all other *cis*-[PtA$_2$(nucleotide)$_2$] solid-state structures: a ΛHT conformation, very strong hydrogen-bond interactions between the phosphate and N1H of *cis* nucleotides, and a very small dihedral angle between the planes of the two guanines lying nearly perpendicular to the coordination plane. These new results indicate that, because there are no local base–base repulsions precluding the ΛHT conformer, global forces rather than local interactions account for the predominance of the ΔHT conformer over the ΛHT conformer in the solid state and in both inter- and intrastrand HT crosslinks of oligonucleotides and DNA.

Keywords: antitumor agents · chiral resolution · metal–nucleotide interactions · platinum · X-ray diffraction

[a] Prof. G. Natile
Dipartimento Farmaco-Chimico, Università degli Studi di Bari
Via E. Orabona 4, 70125 Bari (Italy)
Fax: (+39) 080-544-2230
E-mail: natile@farmchim.uniba.it

[b] Dr. M. Benedetti
Dipartimento di Scienze e Tecnologie Biologiche ed Ambientali
Università degli Studi di Lecce
Via Monteroni, 73100 Lecce (Italy)

[c] Dr. G. Tamasi, Prof. R. Cini
Dipartimento di Scienze e Tecnologie Chimiche e dei Biosistemi
Università degli Studi di Siena
Via Aldo Moro 2, 53100 Siena (Italy)

[d] Prof. L. G. Marzilli
Department of Chemistry, Louisiana State University
Baton Rouge, LA 70803 (USA)

Supporting information for this article is available on the WWW under http://www.chemeurj.org/ or from the author: CD spectra of [Pt(Me$_4$DAE)(5′-GMP)$_2$] collected at different pH values; ^{1}H NMR shifts for [Pt(Me$_4$DAE)(5′-GMP)$_2$] and [Pt{(*R*,*R*)-Me$_4$DACH}**G**$_2$] and [Pt{(*S*,*S*)-Me$_4$DACH}**G**$_2$] complexes; bond lengths [Å] and angles [°] for Na$_2$[Pt(Me$_4$DAE)(5′-GMP)$_2$]·7H$_2$O (Na$_2$**1**·7H$_2$O) starting from those closer to the metal center; X-ray structural data for *cis*-[PtA$_2$(6-oxopurine)$_2$] compounds, ordered according to decreasing average value of the dihedral angle (Φ) between the purine and the coordination planes; description of electrostatic interactions around the Na cations; list of selected intermolecular hydrogen bonds stabilizing the crystal structure.

Introduction

Cisplatin (*cis*-[$Pt(NH_3)_2Cl_2$]) is an important example of the very widely used *cis*-[PtA_2X_2] drug type (A_2 = two amines or a diamine, X_2 = two monoanions or a dianion).[1–5] Its activity is widely attributed to the formation of adducts involving two guanines in DNA, crosslinked to Pt at the N7 atoms,[1,2,6,7] and the extent of d(GpG) intrastrand crosslinking correlates well with treatment outcomes.[8]

Evidence relying on diverse methods for both solution and solid states, such as X-ray crystallographic and NMR spectroscopic characterizations and enzymatic digestion/gel electrophoresis of conformationally frozen crosslinked adducts, mainly indicates that the two guanine bases are head-to-head (HH, Figure 1).[9–22] However, there is some evidence that head-to-tail (HT) crosslinks form for both intrastrand[9] and interstrand crosslinks.[23,24] Such HT adducts could contribute to anticancer activity, and evidence exists that many Pt compounds incapable of forming the main DNA HH adducts made by cisplatin exhibit anticancer activity.[2,25,26] In DNA and oligonucleotide HT adducts and for all related HT forms characterized by solid-state crystallography, the chirality of the HT conformer typically found is Δ. All known *cis*-[metal(6-oxopurine nucleotide)$_2$] adducts (involving 5′-GMP, 5′-IMP, and their phosphate methyl esters) crystallize in the ΔHT conformation, not only for square-planar Pt with several carrier ligands, but also for examples of square-planar and octahedral complexes of Co, Cu, Zn, Cd, and Pd.[27–43] Also, the Δ conformation is found in all solid-state structures of Pt compounds with G nucleosides.[27–30,32–34,38,41–47] Furthermore, all known structures of *cis*-[metal(6-oxopurine nucleotide)$_2$] adducts in the HH conformation have nucleotides that are linked by a sugar–phosphate backbone.[10,13,14,21,48,49]

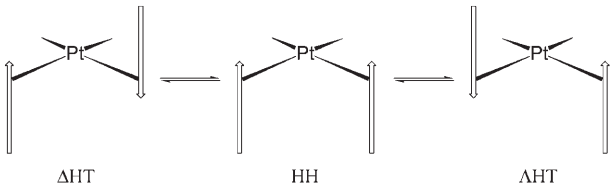

Figure 1. Possible conformers for platinum complexes with *cis* G units (each guanine is represented with an arrow, the tip of which represents a H8 atom). For a head-to-tail (HT) orientation of two guanine units, the Δ or Λ chirality is defined according to the handedness of two straight lines, one perpendicular to the coordination plane and passing through platinum and the other connecting the O6 atoms of the two guanines.[50,51]

By using ligands with bulk in the coordination plane sufficient to reduce dynamic interchange between conformers, but not so bulky as to preclude the existence of the various possible conformers, we have obtained unambiguous evidence that in typical cases all three conformers exist in solution in measurable amounts. The HT conformers are favored over the HH conformer both by lower steric clashes and by better dipole–dipole interactions (the favored HT chirality, Δ or Λ, depends on the carrier ligand and the position of the phosphate group).[52] In addition, the HH conformer is disfavored by clashes of the G O6 atoms.[52,53] Nevertheless, even for adducts with some relatively bulky ligands, the HT conformers are unstable in duplex DNA.[9] Thus, it is the global nature of the overall structure, rather than the local nucleobase–nucleobase interactions, that plays a dominant role in favoring the HH conformer. Also, the dominance of the ΔHT conformer and the scant evidence for the ΛHT conformer in interstrand DNA and in oligonucleotide crosslinked adducts suggest that global factors associated with the backbone disfavor the ΛHT conformer. Stated differently, the typical order of conformer stability observed for adducts with sugar–phosphate backbones (HH > ΔHT > ΛHT) suggests that remote rather than local factors cause this order to deviate from that found for simpler adducts (ΛHT ≈ ΔHT > HH). However, until now, the prevalence of the ΔHT conformer and the absence of a crystallized ΛHT conformer from any laboratory and with any metal introduce some level of uncertainty about the validity of this general conclusion. Specifically, we cannot exclude with a high level of confidence the possibility that unfavorable local base–base or base–sugar interactions between the two *cis* nucleotides disfavor the ΛHT form in the solid state or in adducts that have the nucleotides linked by a sugar–phosphate backbone.

By using both NMR and CD spectroscopic methods,[52,54] we determined that the preference for the ΛHT conformation requires both an N1H on the 6-oxopurine (i.e., the effect decreased markedly if N1 was methylated or deprotonated) and a 5′-phosphate group. NMR data indicated that the 5′-GMP nucleotides maintained the preferred *anti* conformation. Structural models with both 5′-GMP nucleotides in the *anti* conformation suggested that the 5′-phosphates are directed toward the *cis* amines in the ΔHT conformer and toward the *cis* nucleotide in the ΛHT conformer. Therefore, phosphate interactions with the *cis* amine (hydrogen-bond interaction) and with the platinum core (electrostatic interactions) will favor the ΔHT conformer, whereas phosphate interactions with the *cis* guanine (hydrogen-bond interaction with *cis*-5′-GMP N1H)[55–58] will favor the ΛHT conformer. However, even for those cases in which our choice of carrier ligand restricted the rotation about the Pt–N7 bond, these adducts are rendered very dynamic by rapid motions involving rotation about the N9–C1′ and the C4′–C5′ bonds, and interchange among a very broad range of sugar puckers. Factors we identified as favoring the ΔHT conformer found support in several X-ray structures with the ΔHT conformer, but evidence in the solid state to support both the presence of favorable N1H···5′-phosphate interactions and the absence of unfavorable base–base interactions in a ΛHT conformer was totally lacking. Thus, it was a desirable goal to obtain a solid-state structure of a ΛHT conformer.

We reasoned that, although there could be a significant crystal-packing preference for the ΔHT rotamer, we might

be able to crystallize this elusive conformer by choosing those circumstances known from our work to lead to greater stability of the ΛHT conformer. For this, we selected the [Pt(Me_4DAE)(5′-GMP)$_2$] complex (Me_4DAE = *N*,*N*,*N*′,*N*′-tetramethyl-1,2-diaminoethane). The two methyl substituents on each chelate-ring nitrogen were chosen both to eliminate phosphate/*cis* amine hydrogen-bond interactions and to hinder wrapping of the sugar–phosphates around the metal core by preventing oppositely charged moieties from approaching each other closely. These factors destabilize the ΔHT conformer. The bulky Me_4DAE ligand also destabilizes the HH conformer. We employed neutral pH because the phosphate group is fully deprotonated, favoring hydrogen bonding and the ΛHT conformer.[55–58] With this strategy we were able to obtain, for the first time, crystals of a pure ΛHT rotamer, [bis(guanosine-5′-monophosphate(-2))(*N*,*N*,*N*′,*N*′-tetramethyl-1,2-diaminoethane)platinum(II)] disodium salt heptahydrate, Na_2[Pt(Me_4DAE)(5′-GMP)$_2$]·7H_2O, Na_2**1**·7H_2O. The crystallographically determined structure confirmed the importance of the interaction between the *cis* 5′-GMP nucleotides in a ΛHT conformer and has revealed structural features unobtainable by solution methods. Moreover, the faster rate of formation of the [Pt(Me_4DAE)(5′-GMP)$_2$] adduct from [Pt(Me_4DAE)(H_2O)$_2$]$^{2+}$ and 5′-GMP relative to that of the atropisomerization rate allowed us to establish that the ΔHT rotamer is kinetically preferred and the ΛHT rotamer is thermodynamically preferred.

Results

Synthesis and spectroscopic characterization: The [Pt(Me_4DAE)(5′-GMP)$_2$] adduct was obtained by reaction of [Pt(Me_4DAE)(H_2O)$_2$]SO_4 with Na_2(5′-GMP) in a 1:2 molar ratio (pH ≈ 3–3.5 and T = 22 °C). The ^{1}H NMR spectrum exhibits four new H8 peaks 1 h after mixing. During the course of the reaction there was a steady decrease of the H8 peak of free 5′-GMP and a steady increase of two of the new H8 peaks (at 8.44 and 8.42 ppm). The other two new H8 peaks (at 8.714 and 8.709 ppm) have their highest intensities early in the reaction and then decrease to zero (Figure 2).

From the time dependence, the peaks near 8.71 ppm are undoubtedly from the monoadduct, [Pt(Me_4DAE)(D_2O)(5′-GMP)]. Sketches of the two rotamers of the monoadduct (Figure 3), with the Me_4DAE placed in the rear and the 5′-GMP nucleobase placed at the left-hand coordination site, illustrate that only two rotamers are possible because the Me_4DAE ligand is symmetrical. Two sets of resonances can be observed for the monoadduct only if the two rotamers interconvert slowly on the NMR timescale. The two rotamers of the monoadduct are named (pro-ΔHT and pro-ΛHT) in relation to the Δ or Λ chirality of the HT conformer that is formed upon coordination of a second G base (in place of the water molecule) in an HT orientation with respect to the pre-existing G. The intensity ratio between the two H8 signals close to 8.71 ppm did not change with time, indicating that the rotamer composition of the monoadduct is under thermodynamic control.

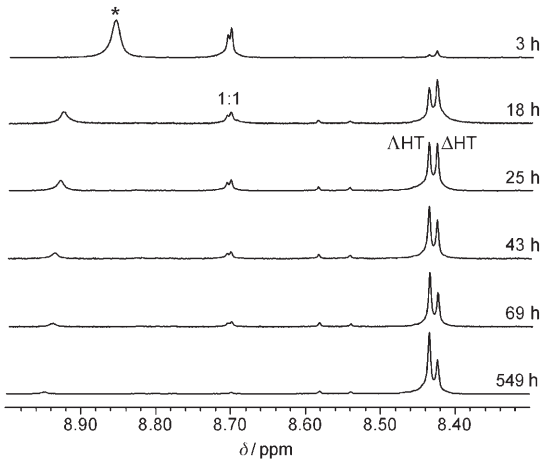

Figure 2. Reaction of [Pt(Me_4DAE)(D_2O)$_2$]$^{2+}$ with 5′-GMP at pH ≈ 3 and 22 °C. ^{1}H NMR spectra were recorded at different time intervals (hours). Peaks of free 5′-GMP (*), monoadduct (1:1), and bisadduct (ΔHT and ΛHT) are labeled.

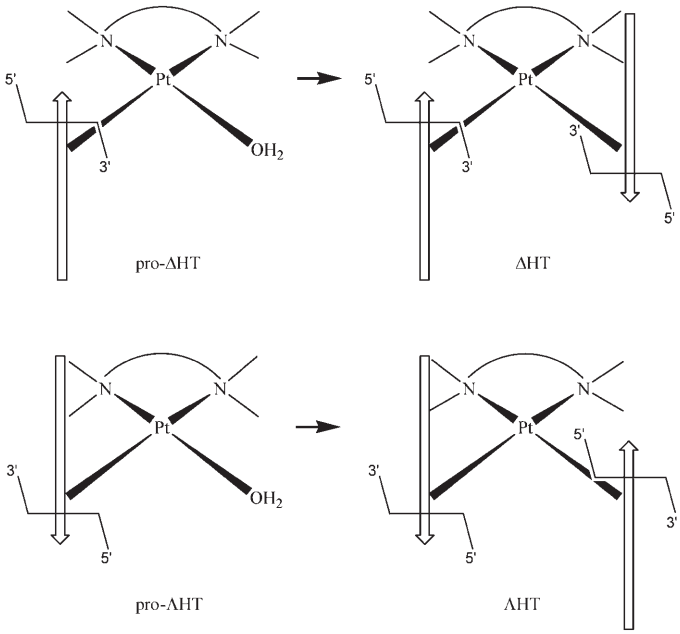

Figure 3. Sketches of the two possible rotamers for the monoadduct (pro-ΔHT and pro-ΛHT) and the two HT conformers of the bisadduct (ΔHT and ΛHT). Arrows represent the G bases, with the tip of the arrow representing a H8 atom. Each rotamer of the monoadduct is named according to the chirality of the bisadduct conformer, which is formed by coordination of a second G unit in an HT orientation with respect to the pre-existing guanine.

The two H8 signals at 8.44 and 8.42 ppm are assigned to [Pt(Me_4DAE)(5′-GMP)$_2$]. This bisadduct has three possible rotamers: two head-to-tail (ΛHT and ΔHT) and one head-to-head (HH), as already shown in Figure 1. Each HT rotamer (C_2 symmetry) will give one H8 ^{1}H NMR signal. For

the HH rotamer (C_1 symmetry), the two G bases are not equivalent; therefore, two H8 signals (of equal intensity) are expected. The two H8 signals at 8.44 and 8.42 ppm have unequal intensities; thus, they must belong to the two HT rotamers. There are, however, two very weak signals of essentially equal intensity at 8.59 and 8.54 ppm that probably belong to the HH rotamer. Throughout the experiment, these signals remain very small, indicating that any HH conformer present is highly disfavored both kinetically and thermodynamically.

One HT conformer of the bisadduct (H8 at 8.42 ppm) is initially more abundant than the other (H8 at 8.44 ppm). With time, the initially more abundant HT conformer decreases and, at equilibrium, becomes less abundant than the second HT conformer (Figure 2).

The chirality of individual HT conformers was deduced by CD spectroscopy. Common CD features of previously studied *cis*-[$PtA_2\mathbf{G}_2$] adducts ($\mathbf{G}$ = detached guanine-base derivatives) allowed us to establish that the HT conformers make the greatest contribution to the CD spectrum[54,57,59,60] and that HT conformers of opposite chirality (Λ or Δ) also have opposite CD features. Moreover, the CD spectrum of a mixture of conformers is reflective of the dominant conformer in solution. Therefore, in the present case, the CD spectrum of the final solution (spectrum at pH 3.0 in Figure S1 in the Supporting Information) indicates a preference for the ΛHT rotamer at equilibrium (negative features at 209 and 255 nm and positive features at 220 and 285 nm). Therefore, the ΔHT conformer dominates in the early stage of the reaction (ΔHT:ΛHT ratio, calculated from ^{1}H NMR spectra at 3 h reaction time, of approximately 70:30; kinetically controlled composition), whereas the ΛHT conformer dominates at equilibrium (ΔHT:ΛHT ratio of 35:65; thermodynamically controlled composition).

The CD spectra of [$Pt(Me_4DAE)(5'\text{-}GMP)_2$] solutions equilibrated at various pH values (Figure S1) also indicate that the intensity of the CD features is greatest at pH 6.5–7.0, at which complete deprotonation of the phosphates occurs (ΔHT:ΛHT ratio of 25:75 as calculated from NMR data) and decreases both at lower pH (reflecting the extent of protonation of the phosphate groups) and at higher pH (reflecting the extent of guanine N1H deprotonation).

A single crystal of Na_2[$Pt(Me_4DAE)(5'\text{-}GMP)_2$], dissolved in water, gave a spectrum that is compared in Figure 4 with the spectra of the pure ΔHT rotamers of the [Pt{(*R*,*R*)-Me_4DACH}($5'$-GMP)$_2$] and [Pt{(*S*,*S*)-Me_4DACH}($5'$-GMP)$_2$] (Me_4DACH = *N*,*N*,*N*′,*N*′-tetramethyl-1,2-diaminocyclohexane).[43] The very slow rate of interconversion between rotamers of these three complexes ensures that the measured CD spectra are those of the pure rotamers. As expected from earlier work,[43] the spectra of the two ΔHT rotamers have nearly a mirror relationship to that of the ΛHT rotamer because this change inverts the chirality of the coupled $\pi\rightarrow\pi^*$ electronic transitions of the two purines.

The CD intensities observed for the ΛHT rotamer of **1** are significantly greater than those observed for [Pt{(*R*,*S*,*S*,*R*)-Me_2DAB}($5'$-GMP)$_2$] (Me_2DAB = *N*,*N*′-dimethyl-2,3-diaminobutane), for which also the ΛHT rotamer was by far the dominating conformer in solution (ΛHT > 95 %).[61] We have proposed that the weakness of the latter CD features is caused by the greater "6-in" canting of the purine bases permitted by the smaller steric interaction between the guanine H8 and the *cis* amine (an N–H instead of an N–Me on the same side of the platinum coordination plane).[43] In the limit of complete canting, the bases lie in the platinum coordination plane, and a negligible CD signal is expected.

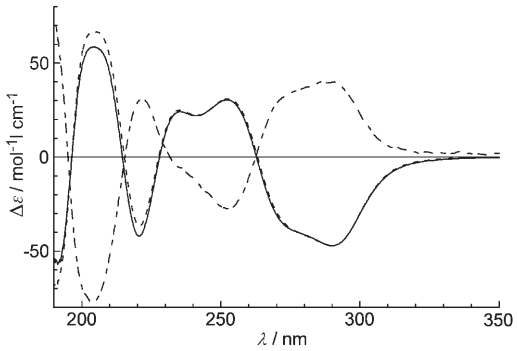

Figure 4. CD spectra of the ΛHT rotamer of [$Pt(Me_4DAE)(5'\text{-}GMP)_2$], **1** (–•–•), and of the ΔHT rotamers of [Pt{(*S*,*S*)-Me_4DACH}($5'$-GMP)$_2$], **2** (– – –), and [Pt{(*S*,*S*)-Me_4DACH}($5'$-GMP)$_2$], **3** (——), taken in D_2O at pH 6.5 (pH value not corrected for deuterium).

From the effect of the guanine anisotropy on the shifts of the *cis* amine N–Me signals, it is possible to identify the chirality of the Me_4DAE chelate-ring pucker of the HT conformers in solution. A correlation exists between the orientation of the guanine and the difference in shifts between geminal N–Me signals. If the six-membered ring of the guanine is on the same side of the coordination plane as the "quasi-equatorial" N–Me, the difference in shift between the two geminal N–Me signals is in the range of 0.18–0.26 ppm. Conversely, if the guanine six-membered ring is on the side of a "quasi-axial" N–Me, the difference in shift between geminal N–Me signals drops to 0.02–0.05 ppm.[62] Relevant values gathered from investigation of [Pt-(Me_4DACH)$\mathbf{G}_2$] complexes of known HT chirality and diamine chelate-ring pucker (this latter determined by DACH chirality) are reported in Table S1. For the [$Pt(Me_4DAE)(5'\text{-}GMP)_2$] adduct, the difference in shift between geminal N–Me signals was in the range of 0.18–0.21 ppm for both the ΛHT and ΔHT rotamers, indicating that the guanine six-membered rings are always on the side of a "quasi-equatorial" N–Me, and, therefore, the pucker of the chelate ring is λ in ΛHT and δ in ΔHT conformers. Our results clearly indicate that the chirality of the HT bases is transmitted to the pucker of the Me_4DAE chelate ring, resulting in nearly complete stereocontrol of the δ or λ chirality of the diamine chelate-ring pucker.

X-ray crystallography: Details of the structure of [$Pt(Me_4DAE)(5'\text{-}GMP)_2$] (**1**) are given in Table 1, with selected bond lengths and angles in Table S2, and the molecular structure appears in Figure 5.

Table 1. Crystal data and structure refinement parameters for Na_2[Pt-(Me_4DAE)(5′-GMP)$_2$]·7H_2O, Na_2**1**·7H_2O.

Parameter	Value
empirical formula	$C_{26}H_{32}D_{24}N_{12}Na_2O_{23}P_2Pt_1$
formula weight	1231.95
T [K]	293(2)
λ [Å]	0.71073
crystal system	monoclinic
space group	C_2 (no. 5)
a [Å]	16.213(2)
b [Å]	10.169(1)
c [Å]	13.877(1)
α [°]	90
β [°]	107.90(1)
γ [°]	90
V [Å^3]	2177.2(4)
Z	2
ρ_{calcd} [Mg m^{-3}]	1.879
μ [mm^{-1}]	3.591
refinement method	full-matrix least-squares on F^2
data/restraints/parameters	2279/10/326
goodness-of-fit on F^2	1.086
final R indices [$I>2\sigma(I)$]	$R1=0.0227$, $wR2=0.0553$
R indices (all data)	$R1=0.0227$, $wR2=0.0553$

Coordination sphere: The metal center sits on a two-fold crystallographic axis and lies exactly in the plane defined by the four donors: the two Me_4DAE nitrogen atoms (N(A)) and the N(7) atoms (N(G)) of the two 5′-GMP nucleotides. The Pt–N(A) and Pt–N(G) bond lengths (2.049(9) and 2.031(9) Å, respectively) and the N(A)-Pt-N(A) and N(G)-Pt-N(G) bond angles (85.7(6) and 82.3(5)°, respectively) are in excellent agreement with the values found for other Pt(II) adducts with *cis* 5′-GMP nucleotides, namely: [Pt-{(*R*,*R*)-Me_4DACH}(5′-GMP)$_2$] (**2**),[43] [Pt{(*S*,*S*)-Me_4DACH}-(5′-GMP)$_2$] (**3**),[43] [Pt(DAP)(Me-5′-GMP)$_2$] (**4**, DAP = 1,3-diaminopropane, Me-5′-GMP = phosphate methyl ester of 5′-GMP),[29] and [Pt(DAE)(5′-GMP)$_2$] (**5**, DAE = 1,2-diaminoethane).[28] The chelate ring of **1** has the δ pucker (opposite to the λ pucker found in aqueous solution) and pure-twist pucker (T, C_2 symmetry, q_2 0.365(1) Å);[63] the value of q_2 is slightly smaller than those found for the Me_4DACH adducts **2** and **3**.[43]

5′-GMP ligands: Geometrical parameters relevant to the purine systems of **1** are in excellent agreement with values previously reported.[28,29] The presence of a proton on N1 is confirmed by the value of 125.2(5)° for the C2-N1-C6 bond angle. The conformation around the N9–C1′ bond is *–anticlinal* (*–ac*) with a torsion angle, χ (C4-N9-C1′-O4′), of –100.6(6)°.

Bond lengths and angles for the ribose moiety of **1** are normal. The endocyclic sugar torsion angles lead to a pseudorotation phase angle (P) of 151.3(2)°, which corresponds to a C2′-*endo* conformation with a small C1′-*exo* component. In contrast, for **2**–**5**, all having the ΔHT conformation, the P values are close to the expected value of 18° for a pure C3′-*endo* form.[28,29,43] As measured at the value of ν_{max}, the ribose pucker in **1** (42.0(2)°) is comparable to those for **2**–**5**.[28,29,43]

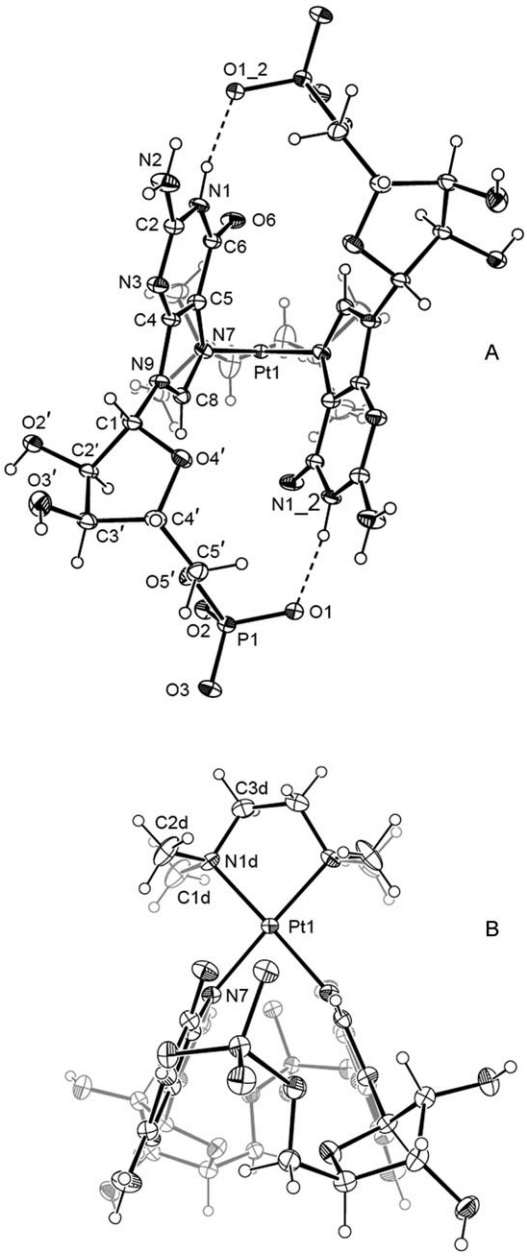

Figure 5. Front view (A) and top view (B) of the complex anion [Pt-(Me_4DAE)(5′-GMP)$_2$]$^{2-}$ (**1**). The ellipsoids enclose 30% probability. The portion of the molecule toward the rear is shown in grey.

Complete phosphate-group deprotonation of **1** is indicated by shorter terminal P–O bond lengths, 1.526(4), 1.508(5), and 1.512(4) Å, relative to P–OH(Me) bond lengths of 1.598(5), 1.576(4), 1.580(2), and 1.536(1) Å in **2**, **3**, **4**, and **5**, respectively.[28,29,43] The bond angles at the phosphorus atom are in the range 102.1(3)–115.1(3)°. Torsion angles α (O3-P1-O5′-C5′, 57.5(2)°), β (P1-O5′-C5′-C4′, –179.7(2)°), and γ O5′-C5′-C4′-C3′, 50.7(2)°) describe the conformations about the P1–O5′, O5′–C5′, and C5′–C4′ bonds as +*gauche* (+*syn-clinal*, +*sc*), pure *trans*, and +*gauche* (+*sc*), respectively.[64]

Relationships between *cis* guanines: In an ideal planar sp^2 N-donor heterocyclic ligand, the nitrogen lone pair forming a bond to the Pt atom lies strictly in the plane of the ligand. In *cis*-[$PtA_2\mathbf{G}_2$] adducts, the two dihedral angles between the plane of each guanine and the coordination plane defined by the four donor atoms (Φ) and the dihedral angle between the planes of the two guanines (Ψ) would all be expected to be close to 90° in the absence of base–base and base–A_2 interligand interactions. The size of Φ in **1** is 80.8(2)°, a value very close to that in **2** (80.9(3)°), but greater than that in **3** (73.2(3)°) and much greater than those found for **4** (53(1)°) and **5** (48(1)°).[28,29,43] In all cases, these compounds have HT base orientations. This orientation is favored by dipole–dipole interactions between the bases, and all past experimental results for small adducts indicate that favorable base–base interactions are accompanied by canting, and that the "6-in" relationship (the six-membered ring of each guanine is leaning toward the *cis* guanine) ensures better dipole–dipole interaction than the "6-out" relationship. We expand on this topic below. Because all five complexes have the "6-in" base relationship, the critical factor restricting the degree of canting (greater canting corresponds to smaller Φ) is the steric interaction between the H8 atom of each guanine and the nearby N-substituent on the *cis* amine. In **1** and **2**, the *cis* amine N−Me substituent on the same side of the coordination plane as the guanine H8 atom has "quasi-equatorial" character, and the values of the nonbonding distance between H8 and the C atom of the *cis*-N-Me (3.378 and 3.138 Å for **1** and **2**, respectively) are close to the sum of the van der Waals radii (3.36 Å) for H (1.20 Å) and CH_3 (2.16 Å).[65] In **3**, the N−Me near the H8 atom has "quasi-axial" character, allowing a greater degree of canting of the guanines before the nonbonding distance of the H8 atom to the *cis*-N-Me C atom reaches a critical value (3.20 Å). Finally, in **4** and **5**, which have no methyl substituents on the *cis*-amine nitrogen atoms, the canting can be much greater without causing a steric clash between the H8 atom and the *cis* amine.

Although **1**, **2**, and **3** all have two methyl substituents on both *cis*-amine nitrogen atoms and small degrees of guanine canting relative to the coordination plane (Φ angles of 80.8(2), 80.9(3), and 73.2(3)° for **1**, **2**, and **3**, respectively), the dihedral angle between the planes of the two guanines (Ψ) in **1** is extremely small (44.2(2)°) relative to the corresponding values for **2** (80.2(3)°) and **3** (78.1(4)°). In **4** and **5**, the Ψ dihedral angle is also rather small (50.2(5) and 49.2(5)°, respectively), but these compounds have a high degree of canting of the guanines (Φ of about 50°), and a narrowing of the Ψ dihedral angle is empirically associated with a high degree of canting of the 6-oxopurines in HT conformers of small *cis*-[metal(6-oxopurine nucleotide)$_2$] complexes, as well as other *cis*-[Pt(6-oxopurine)$_2$] complexes (see Table S3). Compound **1** is a very notable exception, which could be accounted for by the internucleotide interaction described in the following section.

Internucleotide interactions: The ΛHT conformation of the *cis* nucleotides, combined with the *anti* conformation of each nucleotide, directs the sugar–phosphate group of each nucleotide toward the *cis* nucleotide. The resulting positioning is suitable for formation of strong N1−H···O1−P hydrogen bonds in **1** (N···O, 2.689(6) Å; N−H···O, 167(1)°). The two 5′-GMP molecules are linked by two strong hydrogen bonds, creating a pseudomacrocycle.

The X-ray structure of **1** clearly indicates that the C2−NH_2 group adjacent to the N1 atom is not involved in hydrogen bonding with the phosphate. This result is in full agreement with previous observations, indicating that this internucleotide interaction is ruled out if the N1 atom is deprotonated or methylated.[61] Deprotonation of the N1 atom and, to a smaller extent, methylation of the N1 atom could reduce the ability of the adjacent C2−NH_2 group to act as a hydrogen-bond donor. However, the X-ray structure clearly indicates that, probably for steric reasons, the phosphate reaches over the N1H rather than the C2−NH_2. Very likely, the two phosphate/N1H hydrogen bonds tend to bring together the "bottom edges" of the two guanines, whereas the two N7 atoms remain at their normal distance and the N7-Pt-N7 angle in **1** is similar to those of **2** and **3**. The result is a Ψ dihedral angle of 44.2(2)°.

Intermolecular interactions: No intermolecular stacking interactions were found in **1**. The sodium ion is surrounded by seven oxygen atoms: six of these are from four different complex anions and one is from a disordered cocrystallized water molecule (Figure S2). A web of intermolecular hydrogen bonds stabilizes the crystal structure (Table S4).

Discussion

Kinetic versus thermodynamic preference for a given rotamer: The present investigation revealed a kinetic preference for the ΔHT rotamer in the formation reaction of [Pt(Me$_4$DAE)(5′-GMP)$_2$] and a thermodynamic preference for the ΛHT rotamer at equilibrium, whereas the HH conformer was negligibly small throughout the entire experiment. In a previous report on the formation reaction of *cis*-[$PtA_2\mathbf{G}_2$] adducts in which A_2 is a *N*,*N*,*N*′,*N*′-tetramethyl-substituted diamine,[62] we developed hypotheses to explain the high percentages of the ΔHT rotamer observed in early stages of the reaction. In this work, we obtained evidence for a very small amount of the HH rotamer and can now offer a more complete analysis of the kinetic versus thermodynamic preferences.

We previously attributed the very small yield of HH rotamer, a common feature of *cis*-[$PtA_2\mathbf{G}_2$] adducts in which A_2 is a tetraalkyl-substituted diamine, to the inhibition of nucleobase canting by the four N substituents. As a consequence of the low canting, the two O6 oxygen atoms, both electron rich, are constrained to be close to one another in the HH rotamer, a circumstance destabilizing this conformer.[53] In past studies by using A_2 diamines less hindered than tetra-

alkyl-substituted diamines, we found that the HH rotamer was formed as a kinetic product.[55] The new results now allow us to make the following argument, ruling out formation of the HH rotamer as a short-lived transient kinetic product. If the unstable HH product formed initially, it would quickly convert to the HT rotamers. However, the finding that the ΛHT rotamer is favored at equilibrium over the ΔHT rotamer requires that the rate of conversion of the HH rotamer to the ΛHT rotamer be faster than the rate of conversion to the ΔHT rotamer. However, the opposite abundance of HT rotamers is observed. Thus, in this study we establish without question that the HH rotamer is not a significant short-lived transient kinetic product.

Without doubt, the incoming second guanine coordinates in a head-to-tail orientation with respect to the already-bound guanine in the *cis*-[$PtA_2(H_2O)$(5′-GMP)] monoadduct. Thus, a monoadduct having the nucleotide 5′-phosphate directed toward the *cis* amine will lead to a ΔHT bisadduct (pro-ΔHT monoadduct); in contrast, a monoadduct having the nucleotide 5′-phosphate directed toward the *cis*-aqua ligand will lead to a ΛHT bisadduct (pro-ΛHT monoadduct). In the present case of a diamine carrier ligand lacking N protons, the 5′-phosphate can form hydrogen bonds only with the *cis*-aqua ligand in the pro-ΛHT monoadduct. Therefore, the pro-ΛHT monoadduct, stabilized by the phosphate/*cis*-aqua ligand hydrogen bond, is expected to be less reactive than the pro-ΔHT monoadduct, resulting in a kinetic preference for the ΔHT bisadduct. The dominance, at equilibrium, of the ΛHT conformer must stem from a greater thermodynamic stability of this conformer. In the bisadduct end product the 5′-phosphate can form a hydrogen bond only with the N1H atom of the *cis* guanine; this hydrogen bonding is most favorable in the ΛHT rotamer having the 5′-phosphate of each nucleotide directed toward the *cis* guanine. Therefore, the formation of internucleotide hydrogen bonds fully explains why the ΛHT conformer is favored at equilibrium.

"Inverse" transmission of chirality from the HT conformation to the Me_4DAE chelate-ring pucker: A correlation was found in solution between the chirality of the *cis* nucleotides (ΔHT or ΛHT) and the chirality of the chelate-ring pucker (δ or λ). Our explanation for this correlation is the following. As we have already indicated, *cis* guanines in HT conformers tend to be canted "6-in" because this geometry favors dipole–dipole interaction by reducing the H8–O6 distance. The degree of "6-in" canting of the nucleobases, however, is affected by steric repulsion between the H8 atom of each guanine and substituents on the *cis* amine. Moreover, computations indicated that the interaction between the guanine H8 atom and the N–Me of the *cis* amine is slightly greater if the N–Me has "quasi-equatorial" rather than "quasi-axial" character.[43] Because the achiral Me_4DAE ligand has no preference for δ or λ pucker, we can expect that the favored pucker chirality will depend on the steric requirements of the guanine bases of the HT conformer. Therefore, the ΛHT conformer can have the H8 atom on the side of a "quasi-axial" *cis* N–Me, if the Me_4DAE chelate ring adopts a λ pucker. Similarly, the ΔHT rotamer can place the H8 atom on the side of a "quasi-axial" *cis* N–Me if the Me_4DAE ligand has the δ pucker. We found that the guanine six-membered rings are always on the side of a "quasi-equatorial" N–Me, and, therefore, the pucker of the chelate ring is λ in ΛHT and δ in ΔHT conformers. Moreover, because the achiral Me_4DAE ligand can be puckered λ or δ equally well, the degree of "6-in" canting can be similar for ΛHT and ΔHT conformers with no effect upon the relative stabilities of the two conformers. Indeed, we can conclude that in the present case another type of interligand interaction (hydrogen-bond formation between *cis* 5′-GMP nucleotides) is responsible for the greater stability of the ΛHT conformer over the ΔHT conformer.

The direction of conformational chirality transmission (or induction) from bases to carrier ligand just described is the "reverse" of that observed in previously investigated [Pt(CCC)$\mathbf{G}_2$] complexes (CCC = C_2 symmetrical chiral diamine ligand with one hydrogen atom and one alkyl group on each terminal nitrogen). In [Pt(CCC)$\mathbf{G}_2$] complexes the chirality of the diamine induces a preference for one HT conformer (the conformer with the guanine H8 atom on the same side of the coordination plane as the N–H of the *cis* amine being favored because it can be stabilized by greater "6-in" canting of the two guanines). This study of the [Pt(Me_4DAE)(5′-GMP)$_2$] adduct provides the first documented case for such a "reverse" transmission of chirality from the HT guanines in a *cis*-[$PtA_2\mathbf{G}_2$] adduct to diamine chelate-ring-pucker chirality. This finding is further evidence supporting the conclusion that the interaction between the guanine H8 atom and substituents on the *cis* amine is a key factor in determining stability and canting of HT conformers.[52,62,66] For the ΛHT conformer of [Pt(Me_4DAE)(5′-GMP)$_2$], the λ chirality of the diamine pucker found in solution is consistent with established trends, but the δ pucker found in the solid state is opposite to that expected. However, the small Ψ angle coupled with large Φ values in the solid would greatly reduce the interaction between the guanine H8 atom and substituents on the *cis* amine. We shall return to this point below.

Stereochemistry of the complex: All *cis*-[PtA_2(5′-GMP)$_2$] compounds previously characterized in the solid state[28,29,43] were found to have the ΔHT conformation, the conformation that brings each phosphate close to the *cis*-amine.[54,62] We reasoned that tertiary amine ligands, which offset possible phosphate/*cis* amine interactions and hinder wrapping of the sugar–phosphate around the metal core (thus reducing electrostatic interactions between oppositely charged moieties), would destabilize the ΔHT rotamer and offer us better prospects for crystallizing the ΛHT rotamer, the dominant conformer in solution. Crystallization of the ΛHT conformer could also be favored by utilizing neutral pH, at which the phosphates carry a double-negative charge and the ΛHT rotamer of 5′-GMP adducts has the highest stability relative to the ΔHT rotamer.[55,58] Under these conditions, the [Pt(Me_4DAE)(5′-GMP)$_2$] adduct gives a solution composition

of about 75% ΛHT and only 25% ΔHT. This strategy proved to be successful and allowed us to grow X-ray-quality crystals containing the ΛHT conformer. We emphasize the fact that this is not only the first X-ray structure of a ΛHT rotamer of a *cis*-[PtA_2(6-oxopurine nucleotide)$_2$] complex, but also the first case for any *cis*-[metal(6-oxopurine nucleotide)$_2$] complex.

The molecular structure of **1** fully supports the conclusions that were reached in previous work,[52] but were never confirmed by direct evidence, namely, that the ΛHT conformer of *cis*-[PtA_2(5′-GMP)$_2$] complexes are stabilized by phosphate/N1H interactions between *cis*-5′-GMP nucleotides. The X-ray structure reveals that indeed such a hydrogen bond is formed and is quite strong (N···O = 2.692(6) Å, N–H···O = 167(1)°). The C5′-C4′-C3′-O3′ torsion angle is 140.4(7)° in **1** (the ribose has the C2′-*endo* conformation in the S pucker range)[64] and 91.6(1), 78.1(1), 84.5(1), and 85.1(1)° in **2**–**5**,[28,29,43] respectively (the ribose has the C3′-*endo* conformation in the N pucker range).[64] Apparently, an S conformation of the sugar allows the 5′-phosphate to be in a favorable position near the N1H of the *cis* nucleotide.

We emphasize the fact that the C2–NH_2 amino group, although very close to N1H, is not involved in hydrogen bonding with the 5′-phosphate. The hydrogen-bonding pattern is fully consistent with solution studies.[54] We attribute this pattern to the greater acidity of the N1H atom (which renders this group a better hydrogen-bond donor), the favorable position of the N1H atom as revealed by the structure, and the more remote location of the amino group (not easily approached by the 5′-phosphate group).

The most remarkable and noteworthy structural feature of compound **1** investigated here is the combination of a small dihedral angle between the planes of the two guanines ($\Psi = 44.2(2)°$) in a compound with little base canting. This result contrasts with the normal parallel relationship between Φ and Ψ angles (see below and Table S3). To appreciate the commonly found interrelationship between Φ and Ψ values, it is useful to consider the following gedanken experiment. Starting from Φ and Ψ values of 90°, we decrease the Φ angle of both guanines simultaneously to zero. The Ψ angle will also decrease and, in the extreme case of $\Phi = 0°$, Ψ would also equal 0° (this situation corresponds to two interpenetrating guanines lying in the coordination plane). The latter limiting guanine-base positioning, however, can never be reached because the two guanines cannot penetrate each other. The combinations of Φ/Ψ values found for compounds with primary diamines **4** and **5** appear to approach the lowest possible limits that can be reached in experimental systems. An important consideration is that the strong and favorable Pt–N7 bond length of approximately 2.0 Å forces the N7 atom of each guanine and the nearby atoms to be close to each other. The distance between the bound guanine N7 atoms is generally relatively invariant from compound to compound at about 2.9 Å. To relieve the steric interactions of the nonbonded atoms in adducts with a high level of canting, the inner parts of the two guanines have moved apart from each other by bending the Pt–N7 bonds out of the guanine planes, as indicated by the displacement of around 0.55 Å of the platinum atom from the plane of each guanine. Evidently, because this displacement is common in *cis*-[metal(6-oxopurine nucleotide)$_2$] complexes with combinations of low Φ/Ψ value, the balance of forces appears to overcome the unfavorable energy associated with this displacement of the metal from the guanine plane.

In compounds **1**–**3**, the "6-in" canting of the two guanines is strongly inhibited by steric repulsion between H8 of each guanine and N–Me substituents on the *cis* amine; therefore, the Φ values are in the range 73–81°. From the high values of Φ, a comparably high Ψ value would be expected. Indeed, this is the case for **2** and **3**, but not for **1**, which has the low Ψ value of 44.2(2)°. No precedent for the high-Φ, low-Ψ solid-state structure we find for **1** exists among HT conformers of small adducts (see Table S3 for a summary of selected structural features of *cis*-[PtA_2(6-oxopurine)$_2$] HT forms showing the existence of a "quasi-linear" parallel relationship between Φ and Ψ angles).

Examples do exist for high-Φ, low-Ψ solid-state structures in large adducts with guanine bases linked by a phosphodiester backbone.[10,21,67,68] To describe this situation, we conduct a variation of the gedanken experiment, but with no canting. We maintain $\Phi = 90°$ and decrease Ψ. This change would make the base planes more parallel to each other, would keep the bases perpendicular to the coordination plane, and would increase the dipole–dipole interaction in an HT conformer. In the extreme, the bases again would interpenetrate at $\Psi = 0°$. However, because the N7···N7 distance is fixed, this squeezing of the bases together would have unfavorable components. For example, the bond to Pt would no longer be in the guanine plane and several distances between guanines would fall below the typical stacking distance of about 3.4 Å. One driving force for this alternative way to narrow Ψ could be steric repulsion between each guanine and the *cis*-amine Me groups. One might imagine that such steric repulsion in **1** leads to a small value of Ψ. However, in addition to **2** and **3**, there are other examples of compounds in which the bulky ligands are tolerated well and the values of both Ψ and Φ are high (see Table S3). In addition, the unusual δ pucker found in **1** is best understood by lower than normal interactions of the guanine bases with the diamine. Therefore, steric repulsion between each guanine and the *cis*-amine Me groups cannot be responsible for the narrowing of Ψ in compound 1.

We believe that the driving force for the narrowing of the dihedral angle between the guanine planes (Ψ) to 44.2(2)° is provided by the 5′-phosphate/N1H hydrogen-bond interactions between the two *cis*-5′-GMP nucleotides. In other words, the 5′-phosphate of one 5′-GMP can approach more closely the N1H atom of the *cis*-5′-GMP if the "bottom edge" of each six-membered ring of the two guanine nucleobases is close to the other nucleobase. This situation leading to a low Ψ value emanates from the ΛHT conformation in compound **1** because Ψ is much greater (80° compared to

44°) in strictly analogous compounds with tetramethyl-substituted diamines (**2** and **3**) having the ΔHT conformation.

Our finding of a narrow Ψ in a ΛHT conformer makes it very clear that local base–base interactions are not the reason for the lack of previous examples of a ΛHT conformer in the solid state or of the absence, thus far, of a clearly abundant ΛHT conformer of adducts with guanine bases linked by a sugar–phosphate backbone. In the case of **1**, it is very clear that the more remote effect of the 5′-phosphate/N1H *cis* nucleotide hydrogen bond plays an important role, both in favoring the ΛHT conformer and in contributing to factors favoring a small Ψ. In water, the solvent molecules are expected to compete strongly for hydrogen bonding with the phosphates and the N1H atoms and to diminish the importance of electrostatic attraction of the phosphate groups toward Pt. As a consequence, the base/base dihedral angle and the sugar conformation are likely to become "normal" with the result that the NMR chemical shifts and the H1′ coupling constants observed for **1** are similar to those observed for the ΔHT conformer and for **2** and **3** (Table S1), and the CD spectrum of **1** is nearly a mirror image of those of **2** and **3** (Figure 4). Thus, it is likely that the Ψ and Φ values of the ΔHT and ΛHT conformers are similar in solution. These results and our interpretations are clearly consistent with previous observations. For example, several related adducts of a 12mer with several carrier ligands have the HH conformer with little canting and remarkably small Ψ values ($<30°$).[10,21,67,68] These oligonucleotides also have a large segment that is A form. However, once dissolved, the 12mer reverts to B form. Controversy continues about the solution structure of the crosslink, and one of our laboratories has proposed a structural model[11] that has a crosslink very similar to that in a well-defined small d(pGpG) adduct[48] and also in an oligomer bound to a high-mobility group (HMG) protein.[13] However, the dissolution of the 12mer to form a B-form duplex is probably accompanied by an opening of the Ψ from $\approx30°$ to ≈70–80°.

Conclusion

NMR-based solution structural models and X-ray structures have been obtained from studies of *cis*-[$PtA_2\mathbf{G}_2$] and *cis*-[PtA_2(d(XGpGY))] adducts (d(XGpGY) = intrastrand crosslink models with the d(GpG) bound to Pt with or without various phosphate or nucleotide X and Y substituents attached to the 5′ and 3′ residues, respectively). Reported structures have various combinations of values for Φ (dihedral angle between the guanine and coordination planes) and Ψ (dihedral angle between the planes of the two guanines). Because of the dynamic nature of these *cis*-[PtA_2] adducts, metric aspects of the solution structures are uncertain; however, the evidence is overwhelming that even major features of the solid-state structures frequently do not persist in solution. In many previous cases, the structures of adducts were subject to large forces characteristic of the solid state or of large molecules (e.g., oligonucleotides). In the solid state, structures of oligonucleotide adducts are subject to a combination of these forces. Thus, uncertainty remains about the factors influencing structure. However, we report a new structure that has known related compounds, all having carrier ligands with four methyl groups surrounding (and thus "insulating") the [Pt(5′-GMP)$_2$] moiety. The finding that the new adduct (**1**) has high Φ and low Ψ values relative to the closely related adducts (**2** and **3**) with high Φ and high Ψ values allows us to roughly estimate the energy needed to alter the Ψ value. The low Ψ value found here can be reasonably attributed to local forces, such as the two hydrogen bonds in **1**. Although these hydrogen bonds are strong, the energy involved is still rather small. Thus, we conclude that little energy is needed to change the Ψ value dramatically.

Analysis of H8 NMR shifts and CD signal intensities of *cis*-[PtA_2(5′-GMP)$_2$] adducts (**1**, **2**, and **3**) establishes that these compounds have very similar Ψ values in solution. This characteristic Ψ could have the narrow Ψ value found in the solid for **1**, the more open values found in the solid for **2** and **3**, or some intermediate value. The abnormal chelate-ring-pucker chirality found in the solid for **1** strongly suggests that the open value reflects the solution situation. In any case, Ψ must change upon dissolution for at least one of the compounds. Also, the *cis*-[$Pt(NH_3)_2$(d(pGpG))] structure in the solid state has four independent molecules in which Ψ varies over 20°.[48,69,70] From this evidence that Ψ is quite variable, one can imagine that even in solution there is a butterfly-like flapping of the bases between the narrow and open Ψ values. It is reasonable to postulate that the Ψ value may change during the dynamic motions characteristic of the "breathing" of Pt–DNA adducts or during the dynamic processes involved in rotamer interconversion.

Our solution studies with *cis*-[PtA_2(5′-GMP)$_2$] complexes involving several diverse carrier ligands indicate that in many cases the ΛHT conformer is the main rotamer present. However, except for **1**, all related complexes, including other 6-oxopurine nucleotides and other metals, have the ΔHT conformation in the solid state. We conclude that this ΔHT conformation preference is mainly a solid-state effect and that there are no local energetic barriers inhibiting formation of the ΛHT conformer in small adducts. For larger *cis*-[PtA_2(d(XGpGY))] adducts, we conclude that the absence of large amounts of the HT conformers is due to forces involving the sugar–phosphate backbone and the global structural preferences of large molecules.[71] In a recent paper, we evaluated the effects of the diamine carrier ligands upon the form (double-stranded, single-stranded coil, or hairpin-forms) of *cis*-[PtA_2] adducts of a palindromic dodecanucleotide.[9] We found that when the Pt agent was added to the duplex form of the dodecanucleotide, the HH conformer was more highly favored as both as a kinetic and a thermodynamic product than would be expected on the basis of the reactions with single-stranded species; such reactions typically form other conformers.

In past work, we found that the carrier ligand could exert a strong influence on the conformer distribution and that the chirality of the ligand could dictate the chirality of the preferred HT conformer. We also found one case in which the configuration of the asymmetric secondary amine in a carrier ligand isomerized under basic conditions to improve carrier-ligand/guanine-base interactions in a platinum GpG adduct.[78] In the present study, we conclude that the chirality of the HT conformer can be transmitted to the carrier ligand and can induce the ligand to adopt a pucker chirality reflecting the HT chirality. This is the first well-documented case of this "reverse" transmission of pucker chirality.

Finally, we summarize the unique features of compound **1** in comparison to the most similar *cis*-[PtA_2(5′-GMP)$_2$] compounds previously investigated (**2**–**5**) as follows: 1) the Λ conformation of the HT rotamer; 2) the very strong hydrogen-bond interaction between the −2 charged phosphates and the N1H bond of the *cis* nucleotide; 3) the C2′-*endo* conformation of the sugars and; iv) the very small Ψ dihedral angle coupled with large Φ values. We conclude that we can provide a rationale for the observed features of **1** and can use our knowledge of the solution chemistry to prepare suitable crystals containing the elusive ΛHT conformer. However, given the rich features of such adducts and the continued great clinical importance of Pt anticancer drugs, we believe it is important to continue to test this interpretation by seeking additional examples of crystalline derivatives. We note that a crystallographically determined structure of an HH form of a *cis*-[PtA_2(5′-GMP)$_2$], or indeed of any other *cis*-[metal(6-oxopurine nucleotide)$_2$] adduct, has not yet been reported.

Experimental Section

All solvents (Aldrich) and Na_2(5′-GMP) and Me_4DAE (Sigma–Aldrich) were used as received. The Zeise salt (K[Pt(C_2H_4)Cl_3]) was prepared from potassium tetrachloroplatinate and ethylene gas as previously described.[73]

Synthesis of [Pt(Me_4DAE)Cl_2]: Me_4DAE (58 mg, 0.50 mmol) was dissolved in diethyl ether. The ether solution was treated with the Zeise salt (150 mg, 0.39 mmol) and the suspension was stirred for 5 d. The pale-yellow precipitate of KCl and [Pt(Me_4DAE)Cl_2] was transferred onto a filter and washed with abundant ether, to remove excess diamine, then with abundant water, to remove KCl, and was finally dried in a stream of dry air; yield, 146 mg (98%). ^{1}H NMR ([D_6]DMSO): $\delta = 2.90$ (s, 4H; CH_2-N), 2.75 ppm (s, 12H; N-Me); elemental analysis calcd (%) for $C_6H_{16}Cl_2N_2Pt$: C 18.93, H 4.25, N 7.31; found: C 18.87, H 4.42, N 7.26.

Synthesis of [Pt(Me_4DAE)(H_2O)$_2$]SO_4: [Pt(Me_4DAE)Cl_2] (100 mg, 0.26 mmol) was suspended in water (50 mL) and treated with Ag_2SO_4 (82 mg, 0.26 mmol). The mixture was stirred overnight in the dark and the solution filtered to remove AgCl. The solution was heated to 80 °C for 1 h to precipitate any residual AgCl, filtered, and evaporated to dryness under vacuum. Then the solid residue was redissolved in MeOH. After filtration, the solution was taken to dryness under vacuum; then the solid residue was dissolved in water and the solvent was removed under vacuum (this procedure ensures complete removal of MeOH). The pale-yellow residue was the desired [Pt(Me_4DAE)(H_2O)$_2$]SO_4 compound; yield, 92 mg (80%). ^{1}H NMR (D_2O): $\delta = 2.80$ (s, 4H; CH_2-N), 2.79 ppm (s, 12H; N-Me); elemental analysis calcd for $C_6H_{20}N_2O_6PtS$: C 16.25, H 4.55, N 6.32; found: C 16.14, H 4.76, N 6.25.

Solution experiments

Spectroscopic measurements during formation reaction and at equilibrium: Stock solutions of Na_2(5′-GMP) and [Pt(Me_4DAE)(H_2O)$_2$]SO_4 (20–30 mM in D_2O) were prepared and adjusted to pH 3 by addition of dilute D_2SO_4 in D_2O. Aliquots of these stock solutions were transferred into an NMR tube to give a final 5′-GMP:Pt ratio slightly higher than 2 and a concentration of complex in the range of 6–8 mM. The formation of the [Pt(Me_4DAE)(5′-GMP)$_2$] complex was monitored by ^{1}H NMR spectroscopy. At least 128 different scans were acquired to reduce the signal-to-noise ratio.

To collect the UV/Vis and CD spectra at equilibrium, aliquots of the NMR solution were diluted to 4×10^{-5} M by addition of H_2O (containing 50 mM Na_2SO_4 as supporting electrolyte to maintain a constant ionic strength). The pH was adjusted to the desired value by addition of NaOH or H_2SO_4. The temperature was kept constant at 22 °C. At least four scans were acquired to reduce the signal-to-noise ratio in CD spectra.

Samples for crystallization: Stock solutions of Na_2(5′-GMP) and [Pt(Me_4DAE)(H_2O)$_2$]SO_4 (20–30 mM in D_2O) were prepared without pH correction. Aliquots of these stock solutions were transferred into a test tube to give a final 5′-GMP:Pt ratio slightly higher than 2. The concentration of platinum complex was in the range of 8–10 mM. After one week (time sufficient by far to ensure complete formation of the [Pt(Me_4DAE)(5′-GMP)$_2$] complex), the pH of the solution spontaneously reached the value of 6.5. Crystallization of the dominant ΛHT [Pt(Me_4DAE)(5′-GMP)$_2$] rotamer, induced by stratification of absolute ethanol above the water solution (ethanol/water ratio of 5:1, v/v), occurred in about 5 months.

Spectra of the pure ΛHT rotamer: A single crystal of the [Pt(Me_4DAE)(5′-GMP)$_2$] complex was dissolved in about 4 mL of D_2O. The mother solution was divided into two aliquots. The first was inserted into a cylindrical cuvette ($l = 0.5$ cm) and the CD and UV/Vis spectra were immediately collected. To reduce the signal-to-noise ratio about 32 scans were acquired. During the acquisition of the CD and UV/Vis spectra, the second aliquot of the solution was inserted into an NMR tube and the ^{1}H NMR spectrum was recorded. To reduce the signal-to-noise ratio about 1024 scans were acquired. The final spectrum showed the presence of only the ΛHT rotamer.

Spectroscopy: ^{1}H NMR spectra were recorded by using a Bruker Avance dpx300 instrument. CD and UV/Vis spectra were recorded by using a Jasco J-810 spectropolarimeter in the range 200–350 nm.

X-ray diffraction: A colorless single crystal of Na_2[Pt(Me_4DAE)(5′-GMP)$_2$]·7H_2O (Na_2**1**·7H_2O, $0.15\times0.15\times0.10$ mm; because the crystallization was performed in D_2O, the nucleotide-exchangeable protons and those of cocrystallized water molecules are intended to be deuterium atoms) was selected, mounted on a glass capillary, and covered with a thin layer of cyanoacrylate Super Attack glue. The diffraction experiment was performed by using a four-circle Siemens P4 diffractometer and the accurate cell parameters were determined with the least-squares algorithm by using 24 randomly selected high-intensity reflections in the range $12 < 2\theta < 32°$. A total of 2536 diffraction beams (2279 were considered observed) were collected in the range $5 < 2\theta < 50°$. The data set was corrected for the Lorentz-polarization and absorption effects (with the ψ-scan technique) by using the XSCAN[74] and XEMP[75] computer programs. Selected crystallographic data are listed in Table 1; bond lengths and angles are reported in Table S2.

The structure was solved by using the direct methods and Fourier techniques of SHELX97[76] implemented in the WinGX package.[77] The hydrogen atoms of the 5′-GMP and Me_4DAE ligands were located in computed positions through the HFIX and AFIX options of SHELX97. The hydrogen atoms of the cocrystallized water molecules were located through the HYDROGEN program[78] implemented in WinGX. The non-hydrogen atoms were refined anisotropically, whereas all the hydrogen atoms were treated as isotropic and their thermal parameters were restrained to 1.2 times the *U*eq of the atoms to which they are bound. The O−H and H···H bond lengths of the cocrystallized water molecules were restrained to 0.93 ± 0.02 and 1.40 ± 0.04 Å, respectively. The chirality of the sugar moiety for the refined structure was confirmed by the value for the Flack

parameter −0.009(6) and by the known configuration of the starting ligand. The final $R1$ and $wR2$ agreement factors were 0.0227 and 0.0553, respectively, for 2279 observed reflections ($I \geq 2\sigma$). Tables of the crystallographic data, atomic coordinates, thermal parameters, and geometrical parameters were obtained by using the CIFTAB program.[79] All calculations were carried out by using Pentium IV machines with SHELX97, PARST97,[80] and ORTEP32[81] softwares implemented in the WinGX package.

CCDC 618593 contains the supplementary crystallographic data for this paper. These data can be obtained free of charge from the Cambridge Crystallographic Data Centre via www.ccdc.cam.ac.uk/data_request/cif.

Acknowledgements

The Ministero dell'Università e della Ricerca Scientifica e Tecnologica (MURST, Roma, Prin 2004 no. 2004059078 006), the Universities of Bari and Siena (ex 60% funds), the Consorzio Interuniversitario di Ricerca in Chimica dei Metalli nei Sistemi Biologici (CIRCMSB), Bari, the EC (COST Chemistry projects D39/0004/06), and NIH Grant GM 29222 to L.G.M. are acknowledged for support. We gratefully acknowledge the following individuals: Dr. F. Berrettini at Centro Interdipartimentale di Analisi e Determinazioni Strutturali (CIADS), University of Siena, for the X-ray data collection; Dr. F. Cannito of CIRCMSB for assistance in manuscript preparation, and Dr. Patricia Marzilli, LSU, for helpful comments and suggestions.

[1] D. Wang, S. J. Lippard, *Nat. Rev. Drug Discovery* **2005**, *4*, 307–320.
[2] M. A. Fuertes, C. Alonso, J. M. Perez, *Chem. Rev.* **2003**, *103*, 645–662.
[3] R. B. Weiss, M. C. Christian, *Drugs* **1993**, *46*, 360–377.
[4] D. Lebwohl, R. Canetta, *Eur. J. Cancer* **1998**, *34*, 1522–1534.
[5] E. Wong, C. M. Giandomenico, *Chem. Rev.* **1999**, *99*, 2451–2466.
[6] *Cisplatin: Chemistry and Biochemistry of a Leading Anticancer Drug* (Ed.: B. Lippert), Wiley-VCH, Weinheim, **1999**.
[7] A. M. J. Fichtinger-Schepman, J. L. van der Veer, J. H. J. den Hartog, P. H. M. Lohman, J. Reedijk, *Biochemistry* **1985**, *24*, 707–713.
[8] E. Reed, R. F. Ozols, R. Tarone, S. H. Yuspa, M. C. Poirier, *Proc. Natl. Acad. Sci. USA* **1987**, *84*, 5024–5028.
[9] V. Beljanski, J. M. Villanueva, P. W. Doetsch, G. Natile, L. G. Marzilli, *J. Am. Chem. Soc.* **2005**, *127*, 15833–15842.
[10] B. Spingler, D. A. Whittington, S. J. Lippard, *Inorg. Chem.* **2001**, *40*, 5596–5602.
[11] L. G. Marzilli, J. S. Saad, Z. Kuklenyik, K. A. Keating, Y. Xu, *J. Am. Chem. Soc.* **2001**, *123*, 2764–2770.
[12] S. M. Cohen, S. J. Lippard, *Prog. Nucleic Acid Res. Mol. Biol.* **2001**, *67*, 93–130.
[13] U.-M. Ohndorf, M. A. Rould, Q. He, C. O. Pabo, S. J. Lippard, *Nature* **1999**, *399*, 708–712.
[14] S. E. Sherman, S. J. Lippard, *Chem. Rev.* **1987**, *87*, 1153–1181.
[15] J. H. J. den Hartog, C. Altona, J.-C. Chottard, J.-P. Girault, J.-Y. Lallemand, F. A. de Leeuw, A. T. M. Marcelis, J. Reedijk, *Nucleic Acids Res.* **1982**, *10*, 4715–4730.
[16] J.-P. Girault, G. Chottard, J.-Y. Lallemand, J.-C. Chottard, *Biochemistry* **1982**, *21*, 1352–1356.
[17] S. O. Ano, F. P. Intini, G. Natile, L. G. Marzilli, *J. Am. Chem. Soc.* **1998**, *120*, 12017–12022.
[18] S. O. Ano, Z. Kuklenyik, L. G. Marzilli in *Cisplatin: Chemistry and Biochemistry of a Leading Anticancer Drug* (Ed.: B. Lippert), Wiley-VCH, Weinheim, **1999**, pp. 247–291.
[19] J. H. J. den Hartog, C. Altona, J. H. van Boom, G. A. van der Marel, C. A. G. Haasnoot, J. Reedijk, *J. Am. Chem. Soc.* **1984**, *106*, 1528–1530.
[20] G. Admiraal, J. L. van der Veer, R. A. de Graff, J. H. J. den Hartog, J. Reedijk, *J. Am. Chem. Soc.* **1987**, *109*, 592–594.
[21] P. M. Takahara, A. C. Rosenzweig, C. A. Frederick, S. J. Lippard, *Nature* **1995**, *377*, 649–652.
[22] A. Gelasco, S. J. Lippard, *Biochemistry* **1998**, *37*, 9230–9239.
[23] H. Huang, L. Zhu, B. R. Reid, G. F. Drobney, P. B. Hopkins, *Science* **1995**, *270*, 1842–1845.
[24] F. Paquet, C. Perez, M. Leng, G. Lancelot, J.-M. Malinge, *J. Biomol. Struct. Dyn.* **1996**, *14*, 67–77.
[25] G. Natile, M. Coluccia in *Metal Ions in Biological Systems, Vol. 42* (Eds.: A. Sigel, H. Sigel), Marcel Dekker, New York, Basel, **2004**, pp. 209–250.
[26] Y. Najajreh, D. Prilutski, Y. Ardeli-Tzaraf, J. M. Perez, E. Khazanov, Y. Barenholz, J. Kasparkova, V. Brabec, D. Gibson, *Angew. Chem.* **2005**, *117*, 2945–2947; *Angew. Chem. Int. Ed.* **2005**, *44*, 2885–2887.
[27] R. Bau, R. W. Gellert, S. M. Lehovec, S. Louie, *J. Clin. Hematol. Oncol.* **1977**, *7*, 51–62.
[28] K. J. Barnham, C. J. Bauer, M. I. Djuran, M. A. Mazid, T. Rau, P. J. Sadler, *Inorg. Chem.* **1995**, *34*, 2826–2832.
[29] L. G. Marzilli, P. Chalipoyil, C. C. Chiang, T. J. Kistenmacher, *J. Am. Chem. Soc.* **1980**, *102*, 2480–2482.
[30] T. J. Kistenmacher, C. C. Chiang, P. Chalipoyil, L. G. Marzilli, *J. Am. Chem. Soc.* **1979**, *101*, 1143–1148.
[31] S. K. Miller, D. G. VanDerveer, L. G. Marzilli, *J. Am. Chem. Soc.* **1985**, *107*, 1048–1055.
[32] "Trace Elements in the Pathogenesis and Treatment of Inflammation", B. deCastro, T. J. Kistenmacher, L. G. Marzilli, *Agents Actions Suppl.* **1981**, *8*, 435–464.
[33] T. J. Kistenmacher, C. C. Chiang, P. Chalilpoyil, L. G. Marzilli, *Biochem. Biophys. Res. Commun.* **1978**, *84*, 70–75.
[34] J. M. Rosenberg, N. C. Seeman, R. O. Day, A. Rich, *J. Mol. Biol.* **1976**, *104*, 145–167.
[35] C. C. Chiang, T. Sorrell, T. J. Kistenmacher, L. G. Marzilli, *J. Am. Chem. Soc.* **1978**, *100*, 5102–5110.
[36] M. D. Poojary, H. Manohar, *J. Chem. Soc. Chem. Commun.* **1982**, 533–534.
[37] D. M. L. Goodgame, I. Jeeves, C. D. Reynolds, A. C. Skapski, *Nucleic Acids Res.* **1975**, *2*, 1375–1380.
[38] R. E. Cramer, P. L. Dahlstrom, *J. Clin. Hematol. Oncol.* **1977**, *7*, 330–337.
[39] R. E. Cramer, P. L. Dahlstrom, M. J. T. Seu, T. Norton, M. Kashiwagi, *Inorg. Chem.* **1980**, *19*, 148–154.
[40] R. W. Gellert, R. Bau, *J. Am. Chem. Soc.* **1975**, *97*, 7379–7380.
[41] H.-K. Choi, A. Terzis, R. C. Stevens, R. Bau, R. Haugwitz, V. L. Narayanan, M. Wolpert-DeFilippes, *Biochem. Biophys. Res. Commun.* **1988**, *156*, 1120–1124.
[42] M. Mikola, K. D. Klika, J. Arpalahti, *Chem. Eur. J.* **2000**, *6*, 3404–3413.
[43] M. Benedetti, G. Tamasi, R. Cini, G. Natile, *Chem. Eur. J.* **2003**, *9*, 6122–6132.
[44] A. Sinur, S. Grabner, *Acta Crystallogr. Sect. C* **1995**, *51*, 1769–1772.
[45] S. Grabner, J. Plavec, N. Bukovec, D. Di Leo, R. Cini, G. Natile, *J. Chem. Soc. Dalton Trans.* **1998**, 1447–1451.
[46] J. D. Orbell, M. R. Taylor, S. L. Birch, S. E. Lawton, L. M. Vilkins, L. J. Keefe, *Inorg. Chim. Acta* **1988**, *152*, 125–134.
[47] H.-K. Choi, S. K.-S. Huang, R. Bau, *Biochem. Biophys. Res. Commun.* **1988**, *156*, 1125–1129.
[48] S. Sherman, D. Gibson, A. Wang, S. J. Lippard, *Science* **1985**, *230*, 412–417.
[49] J. H. J. den Hartog, C. Altona, G. A. van der Marel, J. Reedijk, *Eur. J. Biochem.* **1985**, *147*, 371–379.
[50] R. E. Cramer, P. L. Dahlstrom, *J. Am. Chem. Soc.* **1979**, *101*, 3679–3681.
[51] R. E. Cramer, P. L. Dahlstrom, *Inorg. Chem.* **1985**, *24*, 3420–3424.
[52] G. Natile, L. G. Marzilli, *Coord. Chem. Rev.* **2006**, *250*, 1315–1331.
[53] M. Trani, F. Cannito, G. Natile, P. A. Marzilli, L. G. Marzilli, *Eur. J. Inorg. Chem.* **2005**, 2826–2835.
[54] H. C. Wong, K. Shinozuka, G. Natile, L. G. Marzilli, *Inorg. Chim. Acta* **2000**, *297*, 36–46.
[55] S. O. Ano, F. P. Intini, G. Natile, L. G. Marzilli, *Inorg. Chem.* **1999**, *38*, 2989–2999.

[56] K. M. Williams, L. Cerasino, F. P. Intini, G. Natile, L. G. Marzilli, *Inorg. Chem.* **1998**, *37*, 5260–5268.
[57] H. C. Wong, F. P. Intini, G. Natile, L. G. Marzilli, *Inorg. Chem.* **1999**, *38*, 1006–1014.
[58] J. S. Saad, T. Scarcia, G. Natile, L. G. Marzilli, *Inorg. Chem.* **2002**, *41*, 4923–4935.
[59] L. G. Marzilli, F. P. Intini, D. Kiser, H. C. Wong, S. O. Ano, P. A. Marzilli, G. Natile, *Inorg. Chem.* **1998**, *37*, 6898–6905.
[60] S. O. Ano, F. P. Intini, G. Natile, L. G. Marzilli, *J. Am. Chem. Soc.* **1997**, *119*, 8570–8571.
[61] J. Saad, T. Scarcia, K. Shinozuka, G. Natile, L. G. Marzilli, *Inorg. Chem.* **2002**, *41*, 546–557.
[62] M. Benedetti, J. S. Saad, L. G. Marzilli, G. Natile, *Dalton Trans.* **2003**, 872–879.
[63] D. Cremer, J. A. Pople, *J. Am. Chem. Soc.* **1975**, *97*, 1354–1358.
[64] W. Saenger in *Principles of Nucleic Acid Structure* (Ed.: C. R. Cantor), Springler-Verlag, New York, **1984**.
[65] A. Bondi, *J. Phys. Chem.* **1964**, *68*, 441–451.
[66] G. Colonna, N. G. Di Masi, L. G. Marzilli, G. Natile, *Inorg. Chem.* **2003**, *42*, 997–1005.
[67] P. M. Takahara, C. A. Frederick, S. J. Lippard, *J. Am. Chem. Soc.* **1996**, *118*, 12309–12321.
[68] A. P. Silverman, W. Bu, S. M. Cohen, S. J. Lippard, *J. Biol. Chem.* **2002**, *277*, 49743–49749.
[69] S. E. Sherman, D. Gibson, A. H.-J. Wang, S. J. Lippard, *J. Am. Chem. Soc.* **1988**, *110*, 7368–7381.
[70] M. Coll, S. E. Sherman, D. Gibson, S. J. Lippard, A. H. J. Wang, *J. Biomol. Struct. Dyn.* **1990**, *8*, 315–320.
[71] D. Over, G. Bertho, M.-A. Elizondo-Riojas, J. Kozelka, *J. Biol. Inorg. Chem.* **2006**, *11*, 139–152.
[72] K. M. Williams, T. Scarcia, G. Natile, L. G. Marzilli, *Inorg. Chem.* **2001**, *40*, 445–454.
[73] P. B. Chock, J. Halpern, F. E. Paulik, *Inorg. Synth.* **1990**, *28*, 349–351.
[74] XSCAN User Manual, Siemens Analytical X-ray Instruments, Madison, WI, **1994**.
[75] XEMP Empirical Absorption Correction Program, Siemens Analytical X-ray Instruments, Madison, WI, **1994**.
[76] a) G. M. Sheldrick, SHELXS 97, Program for the Solution of Crystal Structures, University of Göttingen, Göttingen (Germany), **1997**; b) G. M. Sheldrick, SHELXL 97, Program for the Refinement of Crystal Structures, University of Göttingen, Göttingen (Germany), **1997**.
[77] L. J. Farrugia, WinGX, an Integrated System of Windows Programs for the Solution, Refinement, and Analysis of Single Crystal X-ray Diffraction Data, Version 1.64.04, University of Glasgow, **1999**.
[78] M. Nardelli, *J. Appl. Crystallogr.* **1999**, *32*, 563–571.
[79] G. M. Sheldrick, CIFTAB Program for the Preparation of Publication Material, University of Göttingen, Göttingen (Germany), **1997**.
[80] M. Nardelli, PARST 97, a System of Computer Routines for Calculating Molecular Parameters from Results of Crystal Structure Analyses, University of Parma, **1997**.
[81] C. K. Johnson, M. N. Burnett, ORTEP-3 for Windows, Oak Ridge National Laboratory, **1998** (32-bit Implementation by L. J. Farrugia, University of Glasgow).

Received: August 22, 2006
Published online: January 16, 2007

